Frostbite in the Ear

BEE 4530

Computer-Aided Engineering:
Applications to Biomedical Processes

Cornell University

Jacqueline Chiou
Bruno Hortelano
Taylor Macy
Will Weinlandt

Table of Contents

I. Executive Summary

In many polar regions of the Earth, winters are long and cold, and they pose a series of problems to poorly-prepared residents. When walking outside on a cold winter's day, freezing winds induce a high risk of frostbite on all exposed appendages. One of the body parts that is most susceptible to frostbite is the ear, due to its thin slab geometry, highly exposed surface area, location separate from the rest of the body, and the low levels of blood flow that it receives relative to other organs. In order to assess the relationship between the risk of frostbite and different types of wintery weather conditions, COMSOL 4.3b simulations were run for several scenarios.

The geometry of the model consists of a detailed ear and a section of the side of a head. First, a fluid flow analysis was computed, in order to determine the steady state velocity profile of wind moving past and around the ear. Next, a heat transfer simulation was run to calculate the temperatures of the ear. The model was run for both the presence and absence of low speed wind, high speed wind, and sunlight. The goal of this project is to develop a computational model (schematic in Figure 1) describing how quickly frostbite occurs under various conditions, including different wind speeds, air temperatures, and amounts of sunlight.

We computed solutions for different combinations of wind speeds, solar radiation and initial temperatures to determine their effects on frostbite of the ear. The wind speed values used were 1 m/s and 4.47 m/s, the solar radiation values used were 100 W/m^2 and 684 W/m^2, and finally the initial temperatures used were 233 K and 255 K. All combinations of these variables were computed. The parameters and variables of this model can be easily changed to simulate additional environmental factors.

The results, determined by the fraction of the ear that froze, demonstrated that frostbite was most likely to occur when there was higher wind velocity, lower solar radiation, and lower initial air temperature. This shows that, given a constant environmental temperature, the highest risk for frostbite occurs on cloudy days or nights when there are high winds present. The effect of varying each parameter on ear temperature was also determined. Two variables were kept constant while one variable (wind speed, solar radiation or initial air temperature) was changed. The corresponding ear temperature versus time plots for a particular point inside the ear were compared to visualize the effects on changing each of these parameters. The change in solar radiation values caused the most significant difference in ear temperature at a point deep inside the ear. Changes in our wind speed values and initial air temperature values resulted in some difference in ear temperature at a point deep within the ear. But, wind speed is factor that has the greatest effect on the surface temperature of the ear. Therefore, wind speed appears to be the most significant variable when determining frostbite occurrence.

II. Introduction

Anyone who has spent a year in regions with frigid winters knows that poor preparation for harsh winter weather can make any trip outside extremely unpleasant. It can also be dangerous due to the risk of frostbite, a condition that involves the freezing of skin and other tissues close to the surface. Frostbite can cause permanent damage, as the freezing intracellular fluids expand and cause cell lysis (Crawford, et. al., 2013). This condition is accelerated by the body's attempts to protect the vital organs. As the core temperature starts to drop, the cardiovascular system shunts blood flow away from the extremities and towards the core, to minimize heat loss and to ensure that the heart, lungs, and brain remain warm enough to function (Shepherd, et.al., 1983). If the individual does not prevent frostbite and a large amount of tissue is severely frostbitten and then not treated properly, significant amounts of tissue may die. This is dangerous because of gangrene, a condition in which dead tissue becomes infected, and the bacteria quickly spreads to surrounding areas. The main treatment for this condition is amputation of the affected tissues to protect the vital organs (Mayo Clinic, 2014).

There is a risk of frostbite any time the air temperature drops below 0 ºC, but the exposure times that are considered dangerous shorten dramatically once wind is present (NOAA, 2013). This is because the moving air carries heat away from the body more quickly, so a boundary layer of warmer air is unable to form around the individual (Datta and Rakesh, 2010). This results in a sharper temperature gradient that causes heat loss to occur more rapidly.

Although the sun radiates less energy in the winter months, the radiative effects of sunlight can contribute to preventing frostbite. This is especially the case for body parts that have a high surface-to-volume ratio, as the radiation can help to combat the convective heat loss over the same surfaces (Datta and Rakesh, 2010).

III. Problem Statement

Upon examination of databases such as PubMed and Web of Knowledge, no computational models currently exist for frostbite in the human ear. Having a model will allow research to be conducted without the use of physical or animal model systems, and keep people better informed about when, and under which conditions, they should be concerned about frostbite. This model can then be applied to further research on preventing frostbite.

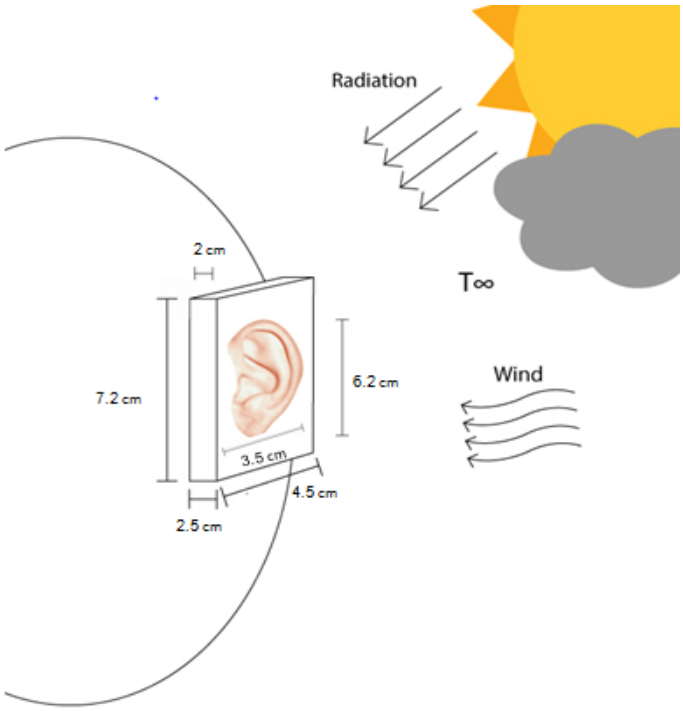

Figure 1: The domain in the box will be modeled in COMSOL to simulate cold air flowing over the human ear and part of the human head. Radiation from the sun will be incorporated into the model through a heat flux term.

IV. Design Objectives and Goals for Finding Frostbite Susceptibility

The proposed model will calculate the amount of time it takes for frostbite to develop in the ear under different circumstances. The ear temperature will be tested under conditions of varying extremes of sun intensity (radiation), wind speed, and air temperature with all possible combinations. In total, there will be eight different tests run using COMSOL using the same exact geometry for each test.

The severity of the different weather conditions will be tested through the creation of a transient, time-varying model of the ear that will provide details about how long it takes for frostbite to occur along with how much of the ear freezes over time.

IV. A. Assumptions:

1) There is heat generation in the section of the head adjacent to the ear, but not in the ear itself, because it does not receive much blood flow, especially due to vasoconstriction (Miller, et. al., 1995).

2) Only a small volume of air around the ear changes temperature due to the heat transfer by convection across the ear. A box with dimensions 5cm x 7 cm x 12 cm will be used to encapsulate this area (Datta and Rakesh, 2010).

3) Every part of the body is initially 37 ˚C until the body is suddenly exposed to the cold air (Vorvick, 2014).

4) The thermal properties of air remain constant with temperature.

5) A temperature dependent apparent specific heat will be used to model the freezing of the ear (Datta and Rakesh, 2010).

6) Air flow around the ear is at steady state, for simplicity.

7) The side head farthest from the ear remains at normal body temperature, 310 K.

8) The bioheat equation is a good model for heat generation in the head, and most of the heat generation in the head is due to blood flow (Datta and Rakesh, 2010).

Table 1: *This table displays the different situations that will be tested by the model (Average Wind Speeds; Russell, 2010; Shelton, 2008).*

Test Run	**Air Temperature (Shelton)**	**Sun Intensity (Russel)**	**Wind Speed (meters/sec.)**
1	-18 °C (~ 0 °F)	684 W/m^2	1 m/s
2	-18 °C	684 W/m^2	4.47 m/s
3	-18 °C	100 W/m^2	1 m/s
4	-18 °C	100 W/m^2	4.47 m/s
5	-40 °C (-40 °F)	684 W/m^2	1 m/s
6	-40 °C	684 W/m^2	4.47 m/s
7	-40 °C	100 W/m^2	1 m/s
8	-40 °C	100 W/m^2	4.47 m/s

IV. B. Goals:

Based on the amount of freezing that occurs in the ear, the most dangerous and the safest environmental circumstances will be determined. The most dangerous situation will have the largest amount of frozen tissue, while the safest situation will have the smallest amount of frozen tissue.

V. Governing Physics for the Ear Model

When people are exposed to the cold winter wind with their ears uncovered, air flows over the slab-like ear, causing a great deal of heat loss by convection (Datta and Rakesh, 2010). The unusual shape of the ear affects airflow around it and needs to be taken into account in the model using the Navier-Stokes governing equations. This air flow will not change much over time, so it can be approximated as steady state flow, and the transient term removed (Datta and Rakesh, 2010).

Heat transfer between the ear and the air needs to be modeled as well, meaning that the Navier-Stokes equations will be coupled with an energy governing equation. This energy equation will include the transient, convection, conduction, and heat generation terms. Meanwhile, there will be transient heat conduction through the cooling ear, since the constantly changing temperatures will affect the rate of conduction through the cooling ear, since the constantly changing temperatures will affect the rate of conduction (Datta and Rakesh, 2010).

The governing equation for the ear-head domain will be a heat transfer equation that includes the transient and conduction terms, with heat generation in the head portion of the domain only (and no heat generation in the ear) due to the limited blood supply that the ear receives (Datta and Rakesh, 2010). This equation will not include convection. Freezing in the ear is modeled by the same heat transfer governing equation, and the freezing is taken into account by the apparent specific heat capacity equation.

<u>Governing Equations</u>

Energy conservation equations for modeling heat transfer:

1) Energy equation of air:

$$\rho_a C_{p,a} \frac{dT}{dt} + \rho_a C_{p,a}\left(v_x \frac{dT}{dx} + v_y \frac{dT}{dy} + v_z \frac{dT}{dz}\right) = k_a\left(\frac{d^2T}{dx^2} + \frac{d^2T}{dy^2} + \frac{d^2T}{dz^2}\right) \quad \text{[Eq. 1]}$$

The Q term represents the heat flux from the Sun's radiation.

2) Energy equation of ear and head:

$$\rho_e C_{p,app,e} \frac{dT}{dt} = k_e\left(\frac{d^2T}{dx^2} + \frac{d^2T}{dy^2} + \frac{d^2T}{dz^2}\right) + Q \quad \text{[Eq. 2]}$$

The heat generation term, Q, is considered to be negligible within the ear because there is minimal blood flow through the appendage at cold temperatures, and not enough circulation to provide heat generation (Shepherd, et. al., 1983). But, heat generation in the head will be considered (using $x < -0.01831$). The convection constants will be determined using the fluid flow equations in COMSOL. Temperature dependent apparent specific heat will be used to take into account the latent heat of fusion when freezing occurs in the ear.

3)Bioheat Equation for Heat Generation in the Head:

$$Q_{blood} = \rho_{blood} \times C_{p,blood} \times \dot{V}_{blood}(T_{body} - T \quad \text{[Eq. 3]}$$

Modeling of Frostbite (Freezing):

$$C_{p,app,e} = (w[(1-f)C_{pu} + fC_{pi} + \lambda_f \frac{df}{dT}] + (1-w)C_{ps}) \quad \text{[Eq. 4]}$$

It is assumed that frostbite begins to occur when the ear temperature reaches about -4 ^oC (Crawford and Zafren, 2013). When the temperature at any point in the ear reaches -4 ^oC, the equation above will be used to model the change in heat of the area of the ear that is at the freezing point. The 'w' term is the fraction of water over the total moisture content (frozen plus unfrozen) in the ear. The 'f' term is the fraction of frozen water over the total moisture content (frozen plus unfrozen) in ear.

Table 2: Material Properties and Constants—The thermal properties of air (subscript a) (Urieli, 2013) and of the ear (subscript e) (Aguilar, et al., 2002; Yu, et. al., 2007) that were found for a temperature of -18 °C. The thermal properties of blood are also used (Elwassif, et al., 2006)

Property	Value
ρ_a	1.385 kg/m^3
C_{pa}	1.003 J/kg*K
k_a	0.02267 W/m*K
ρ_e	1260 kg/m^3
$k_{e,unfrozen}$	2 W/m*K
$k_{e,frozen}$	0.5 W/m*K
ε_e	0.985
C_{pe}	2785 J/kg*K
ρ_{blood}	1060 kg/m^3
$C_{p,blood}$	3600 J/kg*K
	0.004 m^3 blood/m^3 tissue*s
T_{body}	310.15 K

Momentum conservation equations for modeling fluid flow:

$$\rho\left[u\frac{\partial u}{\partial x} + v\frac{\partial u}{\partial y} + w\frac{\partial u}{\partial z}\right] = \mu\left[\frac{\partial^2 u}{\partial x^2} + \frac{\partial^2 u}{\partial y^2} + \frac{\partial^2 u}{\partial z^2}\right] - \frac{\partial P}{\partial x}$$

$$\rho\left[u\frac{\partial v}{\partial x} + v\frac{\partial v}{\partial y} + w\frac{\partial v}{\partial z}\right] = \mu\left[\frac{\partial^2 v}{\partial x^2} + \frac{\partial^2 v}{\partial y^2} + \frac{\partial^2 v}{\partial z^2}\right] - \frac{\partial P}{\partial y} \quad \text{[Eq. 5]}$$

$$\rho\left[u\frac{\partial w}{\partial x} + v\frac{\partial w}{\partial y} + w\frac{\partial w}{\partial z}\right] = \mu\left[\frac{\partial^2 w}{\partial x^2} + \frac{\partial^2 w}{\partial y^2} + \frac{\partial^2 w}{\partial z^2}\right] - \frac{\partial P}{\partial z}$$

Gravity is considered negligible in the momentum conservation equations because convection is much larger than the effect produced by hot air rising (Datta and Rakesh, 2010). If convection were zero, lower density heated air would rise and affect the air flow around the ear (Datta and Rakesh, 2010). This is not the case in our model, since we will not account for natural convection.

Boundary Conditions

For the air domain, the inlet and outlet have the velocity and pressure boundary conditions shown below. All other outer surfaces of the air domain have flux = 0 and a slip boundary condition. Along the head-air interface, there is a no-slip boundary condition.

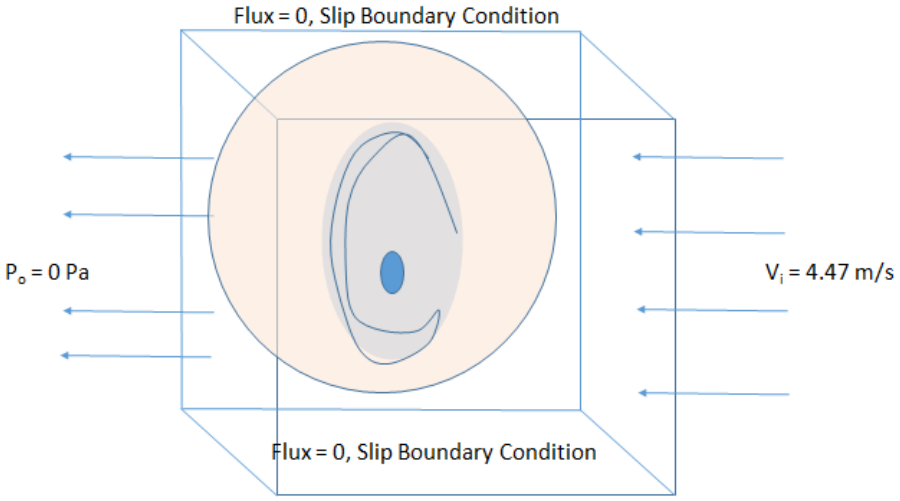

Fig. 2: These are the boundary conditions used to solve the Navier-Stokes equations

The edge of the portion of the head attached to the rest of the body will be perfectly insulated and will always remain at body temperature, 37 °C (310 K).

At the head-body interface: At the head-body interface: $\nabla T = 0, \quad T = 37\ ^{\circ}C$

The temperature of the ear at time zero will be 310K in all eight situations because that is normal body temperature.

$T(t = 0) = 37\ ^{\circ}C$ within the entire ear

The boundary between the ear and the air is an internal boundary and will not be directly defined in COMSOL.

Radiation from the sun will be implemented using a temperature-dependent heat flux term at the surface of the ear with a weak expression: radflux*test(ht.T), where radflux is either 684 W/m^2 or 100 W/m^2.

VI. Results and Discussion

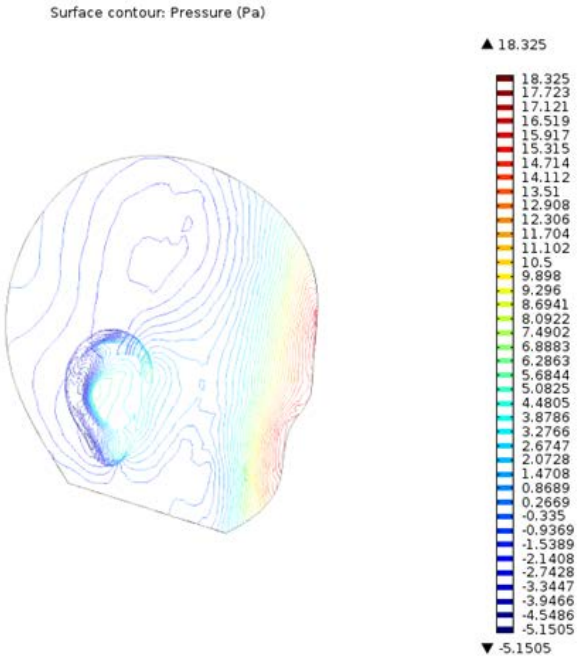

Fig. 3: Pressure contour plot for wind speed of 4.47 m/s

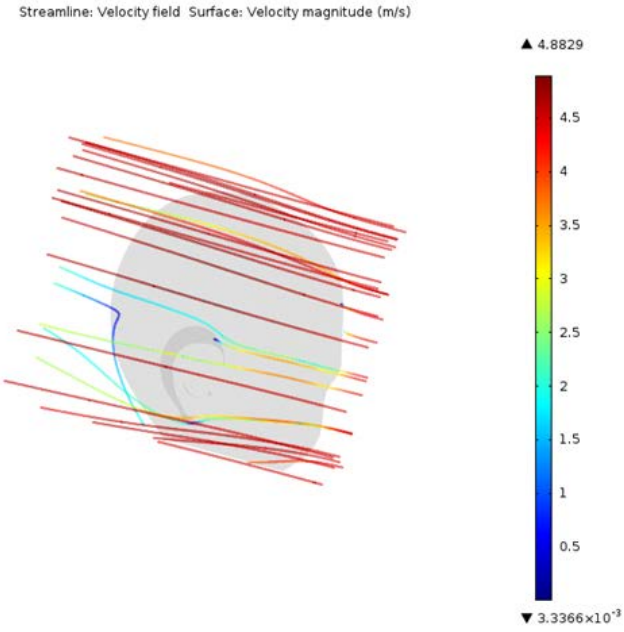

Fig. 4: Velocity streamline plot of wind speed of 4.47 m/s

These are images of the pressure gradient (Fig. 3) and the streamlines (Fig. 4) from our model. On the pressure gradient plot, you can see that there is a smooth gradient from high to low pressure. In Figure 4, there are blue streamlines that show that the air is swirling around behind the ear, at a low speed. More importantly, the light green line following the side of the head shows that there is a higher speed streamline of air near the head that passes just above the top of the ear. This should result in higher convective heat transfer coefficient values, causing more heat loss in these areas. This is verified by the following plots (Fig. 5 and 6).

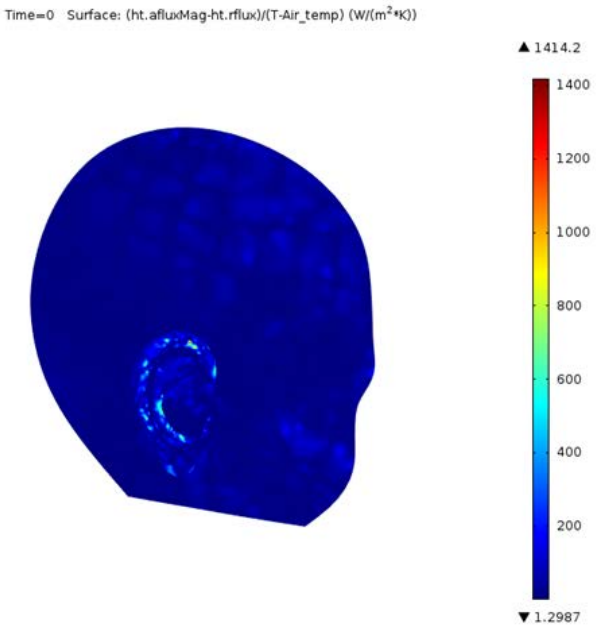

Fig. 5: Plot for convective heat flux in the ear at time = 0 s. Convective heat flux is at a maximum at the top of the ear and on its edges.

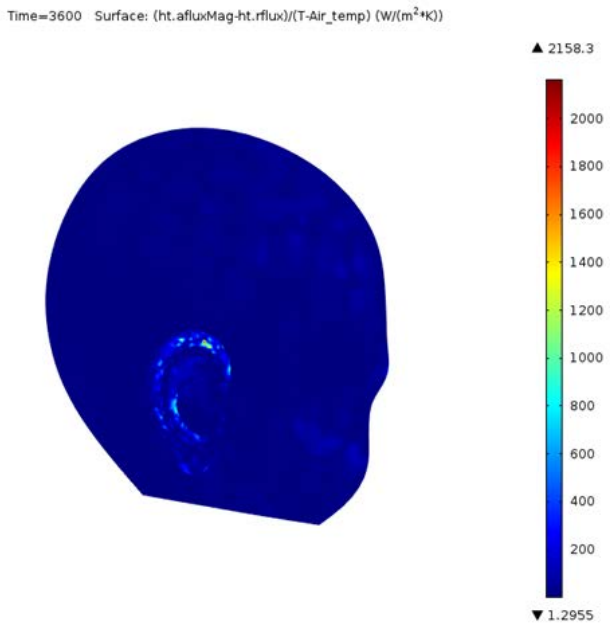

Fig. 6: Plot for convective heat flux in the ear after 1 hour. Convective heat flux is at a maximum at the top of the ear and on its edges, although the convective heat flux appears to be diminished on the sides of the ear.

These areas of higher convective flux display the regions where more heat is lost due to wind. This will correspond to where temperatures drop the most. This is consistent with what is known about frostbite in the ear, because this is the first region of the ear to suffer from frostbite (Pediatric Orthopaedic Society of North America, 2007).

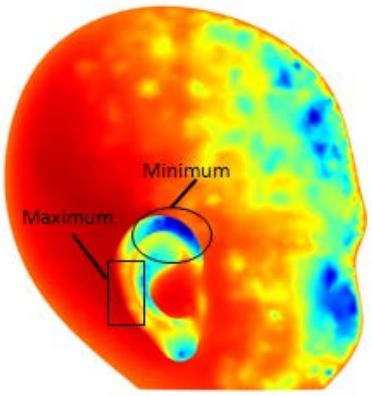

Fig. 7: Plot of the head and ear surface temperatures after 1 hour. The lowest temperatures are on the top of the ear, while the warmest temperatures are on the back side of the ear.

Figure 7 displays the temperatures at the end of our study. Red denotes a higher temperature and blue denotes lower. This temperature graph confirms our hypothesis obtained from the convective heat flux graph. The lower ear temperatures correspond to the areas of highest convective heat flux while the higher ear temperatures correspond to the areas of lowest convective heat flux.

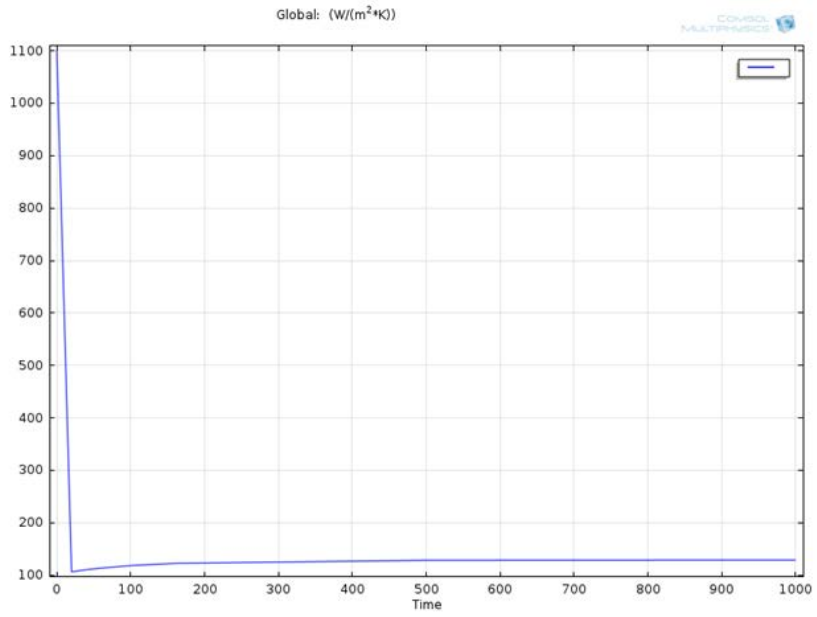

Fig. 8: Plot of the average heat flux over time on the surface the ear at 233 K, 100 W/m^2 , and 4.47 m/s. The heat flux starts off high at the initial time and then drops quickly over time. After the initial drop in heat flux, it can be seen that the heat flux does not change much over time.

This supports what is seen in the other graphs seen below in Sensitivity Analysis (Figures 11-14). The temperature of the ear changes quickly, but then rapidly reaches steady state roughly around 600s. The large initial temperature chance is due to the extremely large temperature difference between the ear and air at the initial time.

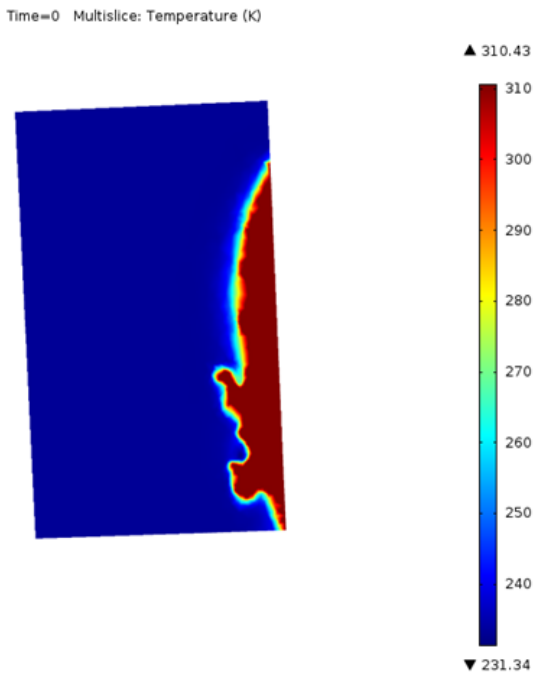

Fig. 9: Slice plot for the ear temperature at time = 0s. This shows

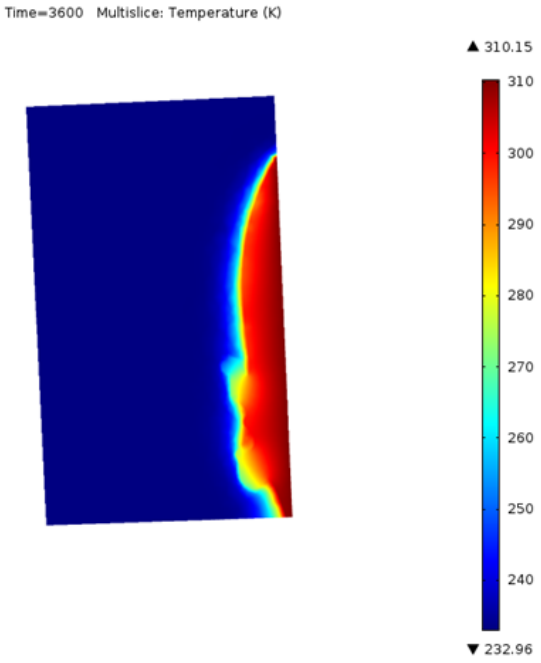

Fig. 10: Slice plot for the ear temperature after an hour. The heat has diffused since the initial temperature, and it can be seen that the ear is coldest on the outside and warmest near the head.

VI. A. Sensitivity Analysis

We tested the different situations seen in Table 1 to see how changing parameters would alter the solution.

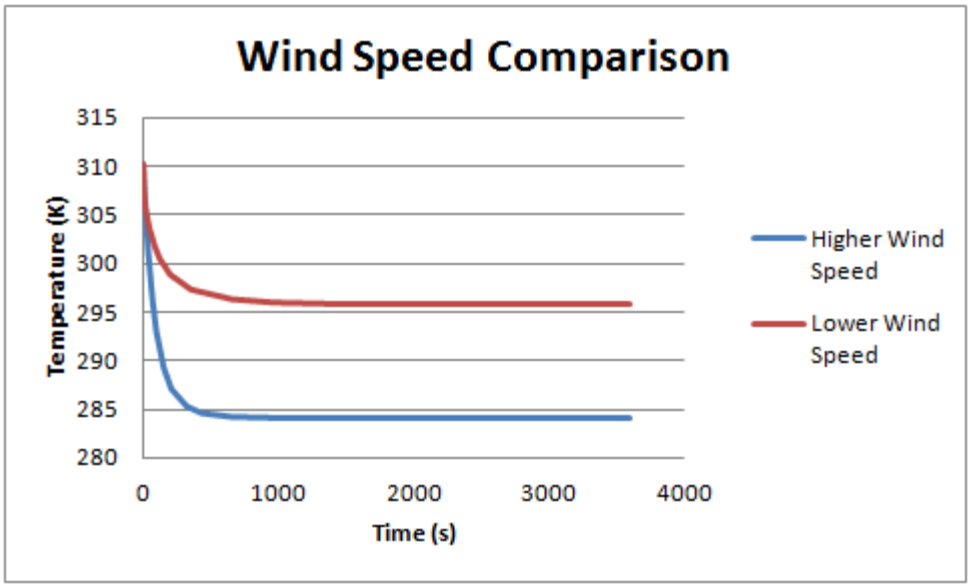

Fig. 11: Temperature vs. Time graph of the ear comparing changes in wind speed. The higher wind speed (4.47 m/s) and the lower wind speed (1 m/s) values were compared while keeping the radiative flux (100 W/m^2) and the initial air temperature (233 K) values constant. There is approximately a 12 K difference in the two steady state ear temperature values.

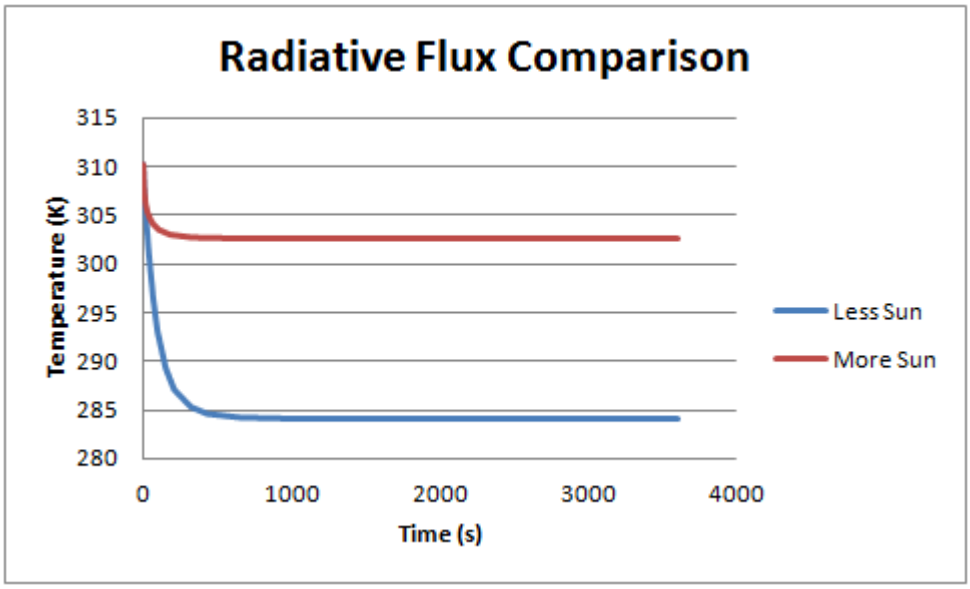

Fig. 12: Temperature vs. Time graph of the ear comparing changes in radiative flux. The radiative flux values for more sun (684 W/m^2) and less sun (100 W/m^2) were compared while keeping the wind speed (4.47 m/s) and the initial air temperature (233 K) values constant. There is approximately a 16 K difference in the two steady state ear temperature values.

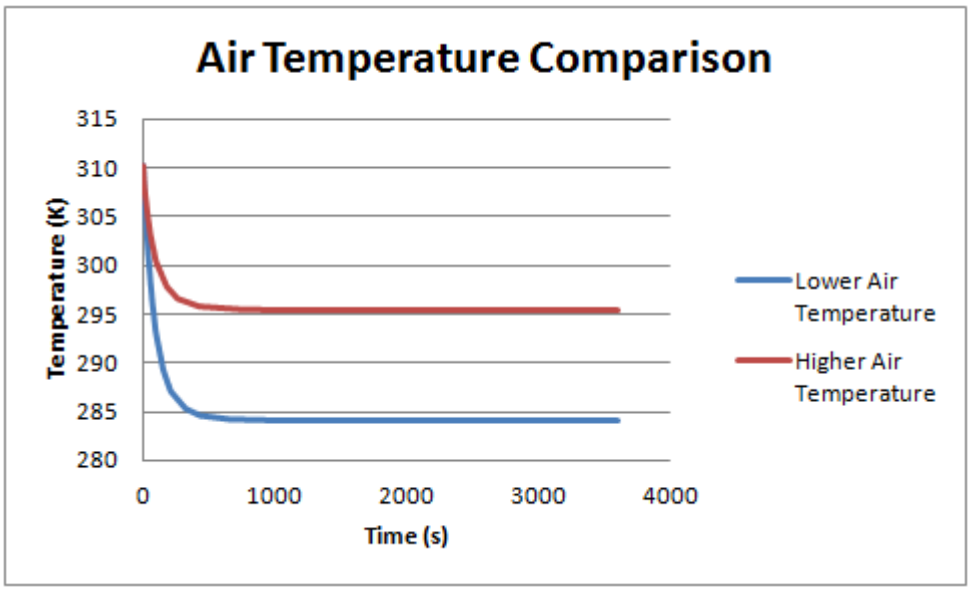

Fig. 13: Temperature vs. Time graph of the ear comparing changes in initial air temperature. The lower initial air temperature (233 K) and the higher initial air temperature (255 K) values were compared while keeping the wind speed (4.47 m/s) and the radiative flux (100 W/m^2) values constant. There is approximately an 11 K difference in the two steady state ear temperature values.

As displayed in Figures 11-13, the greatest change in ear temperature at this point deep inside the ear occurs with our change in radiative flux values. This suggests that the amount of sun affects the likeliness of a person to get frostbite in their ear. The less sun and radiative flux present, the lower the temperature of the ear and the more likely frostbite will occur. The initial air temperature values and the wind speed values do also clearly affect the temperature of the ear, although not as much as the radiative flux values. The change in our wind speed values appears to have a slightly greater effect on ear temperature than the change in our initial air temperature values.

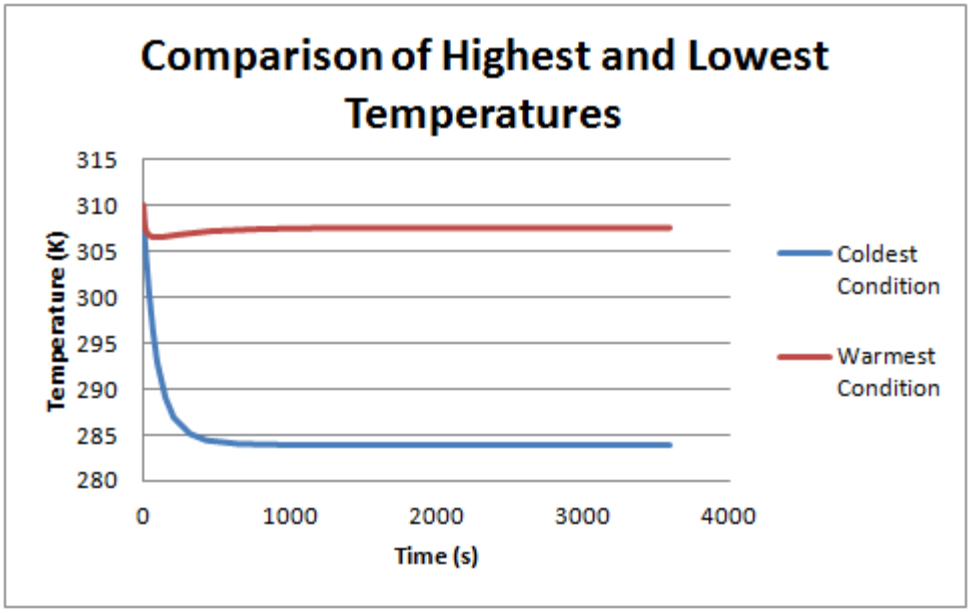

Fig. 14: Temperature vs. Time graph for the ear comparing the overall coldest and warmest environmental conditions. The coldest condition consisted of an initial air temperature of 233 K, a wind speed of 4.47 m/s and a radiative flux value of 100 W/m^2. The warmest condition consisted of an initial air temperature of 255 K, a wind speed of 1 m/s and a radiative flux value of 684 W/m^2.

There is a large difference in the ear temperature over time between these two different conditions. The coldest condition results in a steady state ear temperature that is about 23 K lower than the steady state ear temperature resulting from the warmest condition

Note: The Temperature vs. Time graphs in Figures 11-14 were all calculated at the same point utilized to calculate the temperature domain mesh convergence (-0.01831, 0.007, 0.004), which is deep inside of the ear and not on the surface.

Table 3: This table shows the percent of change in temperature with respect to the percent change in the variable being altered. Based on this, it seems like air temperature change has the largest effect on ear temperature for every percent change in temperature. However, radiative flux has a larger range of values than both temperature and wind speed, so the lack of Sun is still something to be concerned about.

Conditions	**Percent Change**	**New Temperature**	**Temperature Change per Percent Change in Variable**
233 K, 100 W/m^2, 4.47 m/s		284 K	
233 K, 684 W/m^2, 4.47 m/s	584	287 K	0.579%
233 K, 100 W/m^2, 1 m/s	-77.6	296 K	15.1%
255 K, 100 W/m^2, 4.47 m/s	9.44	292 K	81.0%

VI. B. Validation

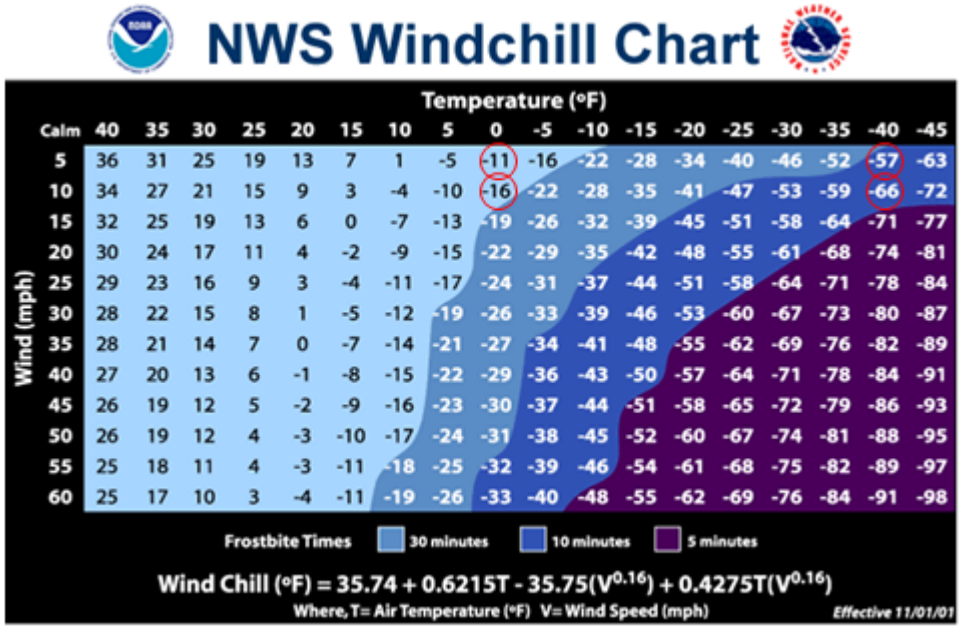

NWS Windchill Chart

Temperature (°F)

Wind (mph)	Calm	40	35	30	25	20	15	10	5	0	-5	-10	-15	-20	-25	-30	-35	-40	-45
5		36	31	25	19	13	7	1	-5	-11	-16	-22	-28	-34	-40	-46	-52	-57	-63
10		34	27	21	15	9	3	-4	-10	-16	-22	-28	-35	-41	-47	-53	-59	-66	-72
15		32	25	19	13	6	0	-7	-13	-19	-26	-32	-39	-45	-51	-58	-64	-71	-77
20		30	24	17	11	4	-2	-9	-15	-22	-29	-35	-42	-48	-55	-61	-68	-74	-81
25		29	23	16	9	3	-4	-11	-17	-24	-31	-37	-44	-51	-58	-64	-71	-78	-84
30		28	22	15	8	1	-5	-12	-19	-26	-33	-39	-46	-53	-60	-67	-73	-80	-87
35		28	21	14	7	0	-7	-14	-21	-27	-34	-41	-48	-55	-62	-69	-76	-82	-89
40		27	20	13	6	-1	-8	-15	-22	-29	-36	-43	-50	-57	-64	-71	-78	-84	-91
45		26	19	12	5	-2	-9	-16	-23	-30	-37	-44	-51	-58	-65	-72	-79	-86	-93
50		26	19	12	4	-3	-10	-17	-24	-31	-38	-45	-52	-60	-67	-74	-81	-88	-95
55		25	18	11	4	-3	-11	-18	-25	-32	-39	-46	-54	-61	-68	-75	-82	-89	-97
60		25	17	10	3	-4	-11	-19	-26	-33	-40	-48	-55	-62	-69	-76	-84	-91	-98

Frostbite Times: 30 minutes; 10 minutes; 5 minutes

$$\text{Wind Chill (°F)} = 35.74 + 0.6215T - 35.75(V^{0.16}) + 0.4275T(V^{0.16})$$

Where, T= Air Temperature (°F) V= Wind Speed (mph)

Effective 11/01/01

Fig. 15: The National Weather Service Windchill Chart shows the freezing times under different environmental situations (NOAA, 2013). Approximates of our four solutions are circled on this chart, with the difference being that 1 m/s is in fact less than 5 mph. This, however, is not a problem because that change would not shift the result's freezing time by much.

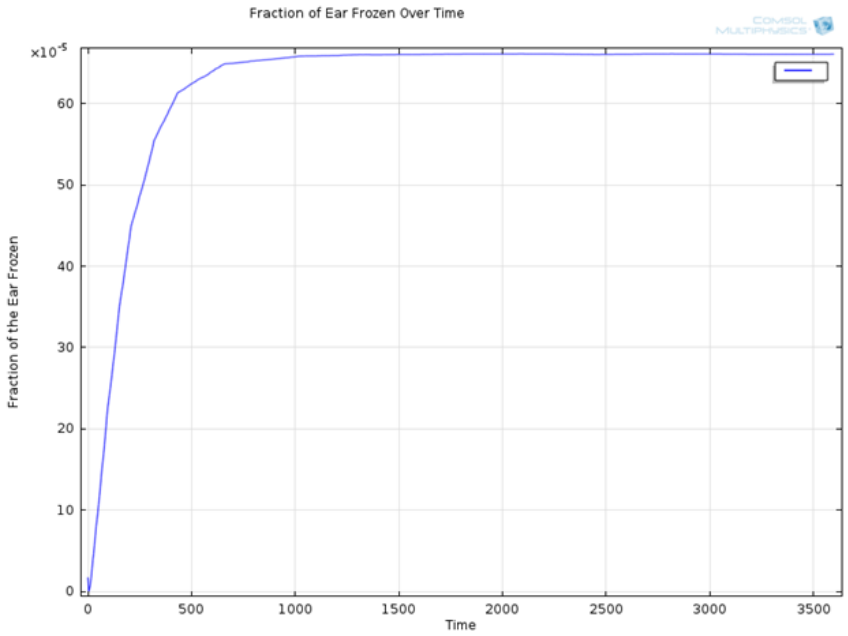

Fig. 16: Fraction of the ear frozen over time for the coldest situation (233 K, 100 W/m^2, and 4.47 m/s). 0.06% of the ear freezes.

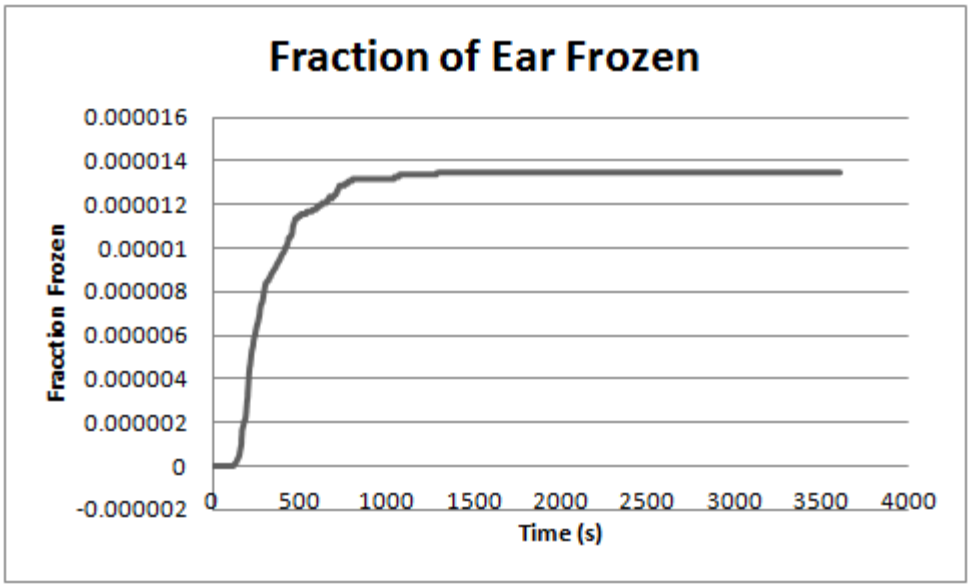

Fig. 17: Fraction of the ear frozen over time for the following situation (255 K, 100 W/m^2, and 4.47 m/s). 0.014% of the ear freezes.

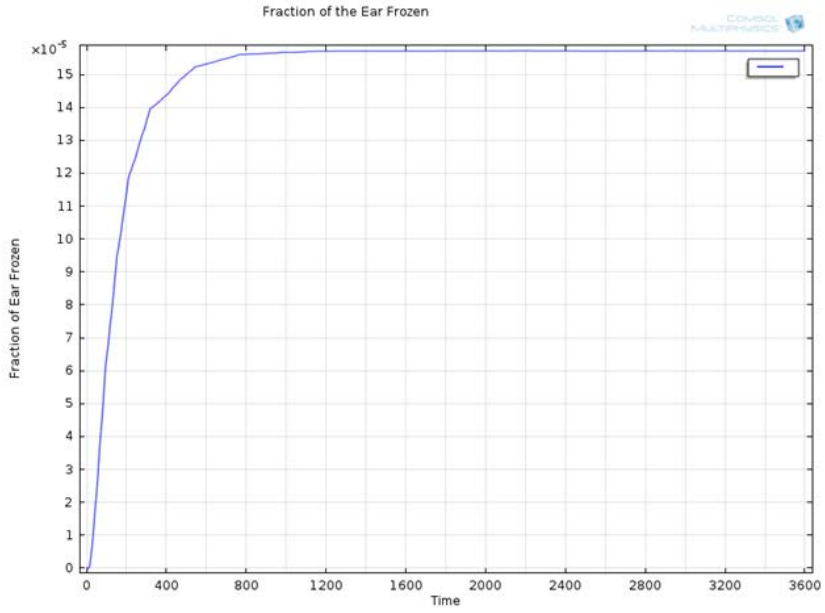

Fig. 18: Fraction of the ear frozen at 233 K, 684 W/m^2, and 4.47 m/s. Steady state is reached at approximately 1200 seconds, and 0.016% of the ear freezes.

Only three of the eight situations result in freezing, according to our model:
233 K, 100 W/m^2, and 4.47 m/s: 0.06% of ear frozen

233 K, 684 W/m^2, and 4.47 m/s: 0.016% of ear frozen
255 K, 100 W/m^2, and 4.47 m/s: 0.014% of ear frozen

The fact frostbite always occurs at a wind speed of 4.47 m/s suggests that a high wind speed (10 mph or more) is the most important factor in determining whether or not frostbite will occur and that higher wind speed has a greater effect than lower radiative heat flux or temperature. It seems that radiative heat flux has the greatest effect on the temperature deep inside the ear, while wind speed has the greatest effect on the temperature on the surface of the ear, because it transfers heat through convection. Also, the increase in radiative flux does not completely nullify the decrease in temperature, since 0.016% of the ear freezes with 233 K, 684 W/m^2, and 4.47 m/s, while 0.014% of the ear freezes with 255 K, 100 W/m^2, and 4.47 m/s.

At a wind speed of 4.47 m/s and a temperature of 233 K, correlating roughly to 10 mph wind and -40 degrees Fahrenheit, a small volume of the ear began freezing very soon after exposure to the air began, and 0.053% of the ear had frozen after 5 minutes.

This is closely related to the National Weather Service (NWS) Windchill Chart prediction under these conditions, which estimates that frostbite will take longer than 30 minutes to occur. When the temperature drops to 233.15 K (-40 degrees Fahrenheit), this chart warns of tissue freezing within 10 minutes of exposure (NOAA, 2013).

Our model shows that a small volume of the ear becomes frozen very quickly after exposure to air, since the outermost layer of the ear is in direct contact with the air. Our model falls right in the ranges provided by the NWS chart because for an air temperature of 233.15 K, most of the sections of the ear that will freeze have already dropped to at least -4 °C (269.15 K), which is the temperature at which the ear generally freezes (Crawford and Zafren, 2013). At 600 seconds (10 minutes), much of the ear that ends up being frozen at steady state has already frozen. It seems like only a very small volume of the ear freezes (see Fig. 10), and that the amount of ear that is frozen reaches steady state within 1 hour of exposure. Of course, this is assuming that the person who is exposed to the cold is not freezing to death. Our model requires the section of the head that we are computing over to be considered independently from the rest of the body. We cannot account for an overall decrease in core body temperature that might conceivably occur if a person is not properly dressed when he is outside in such frigid weather. At the temperatures and duration of freezing we are testing, there is not sufficient time for hypothermia to develop (Crawford and Zafren, 2013).

Interestingly enough, it seems that the National Weather Service has its own computational model for predicting frostbite that incorporates a facial model and heat transfer principles, but we have not been able to find information about this model, aside from the windchill-frostbite chart mentioned. An important point to note is that this chart does not take solar heating into account, as our model does.

VII. Conclusions

We found that the change in radiative heat flux from 100 W/m^2 to 684 W/m^2 due to changes in sun intensity was the variable that had the greatest effect on temperature inside the ear. This can be felt qualitatively anytime one walks outside. Meanwhile, change in wind speed was most important in determining when frostbite would occur, as it affects the surface of the ear. An increase in air temperature influenced the degree of frostbite, but it was not as crucial of a factor as wind speed.

Validation was difficult to find for our model because of our complicated and specific geometry. The one source we found did match our results, although there were discrepancies. Even though the National Weather Service specified that their chart was for their model of a head, we do not know what the exact geometry was. Also, their model did not take into account the radiative flux effects of the sun. If available in the future, more sources for validation will be utilized to ensure that our model is accurate.

A next step towards improving the model is to account for hypothermia. Currently, the model has a boundary condition that sets the inner surface of the head to a constant body temperature of 310 K, and the bioheat generation term assumes that more heat is transferred into the ear as it gets colder, due to the difference in temperature between the blood and tissue. These assumptions are accurate at early times, but not later on, since the body will eventually be unable to maintain normal body temperature after prolonged exposure to the cold. This is one reason that the temperature profile seems to reach steady state rapidly.

Other ways to improve our model would be to include the entire head, or possibly more of the rest of the body, in our geometry. This would make running our model much more time and memory consuming, but it would allow our model to be more physically accurate. Also, adding variation of other factors such as hair, a hat, and earmuffs that cover the head and the ear would allow our model to pertain to a larger variety of people in more situations.

The most important thing to take away from our model and its simulations is that environmental conditions of less sun, cold air temperatures and high wind speeds (especially high wind speeds) warrant taking precautionary measures to prevent the occurrence of frostbite in the ear.

VIII. Appendix A

ε_e = emissivity of the ear
k_e = thermal conductivity of the ear
k_a = thermal conductivity of the air
λ_f = latent heat of fusion of water
$\vec{v}$ = velocity vector
ρ_a = density of air
ρ_e = density of ear
$C_{p,a}$ = specific heat of air
$C_{p,app,e}$ = apparent specific heat of ear
T = temperature
$T_{ambient}$ = air temperature
v_x = air velocity in the x-direction
v_y = air velocity in the y-direction
v_z = air velocity in the z-direction
Q = heat generation in the head only
ρ_{blood} = blood density
$C_{p,blood}$ = specific heat capacity of the blood
$\dot{V}_{blood}$ = volumetric flow rate of blood
T_{body} = body temperature

IX. Appendix B

Table B1: These are the parameter values used for all the runs that were completed for mesh convergence.

Parameter	Value
Air temperature	233.15 K
Wind speed	4.47 m/s
Radiative flux	684 W/m^2

Mesh Convergence:

Mesh convergence was done for Mesh 1 (Stationary mesh) and Mesh 2 (Temperature mesh). For Mesh 1, the velocity was found at a point just outside of the ear (-0.02, -0.0119, -0.03486) in the air domain and the values of velocity were compared for different maximum element size values. For Mesh 2, the temperature at a specific point on the ear-head boundary (-0.01831, 0.007, 0.004) was compared for different maximum element size values. Because of insufficient computing power, solutions were not necessarily calculated with full-converged meshes.

Mesh 1: Final solutions were calculated using the following values
Maximum element size: 0.00695
Minimum element size: 0.001
Number of mesh elements: 174,134

Mesh 2: Final solutions were calculated using the following values
Maximum element size: 0.00675
Minimum element size: 0.001
Number of mesh elements: 240,004

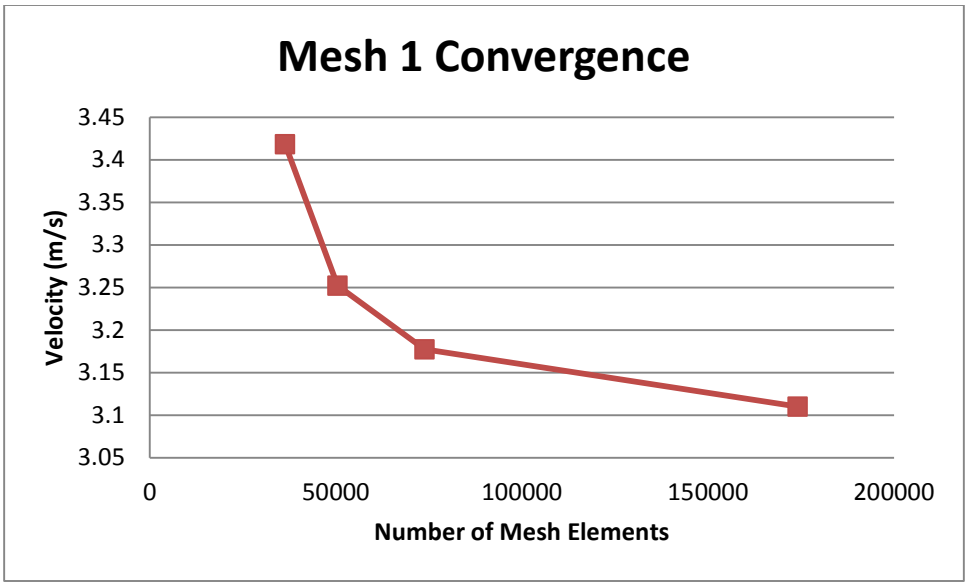

Fig. B1: This shows the mesh convergence for Mesh 1. The mesh is seen to be converging, but solutions could not be obtained for finer meshes due to insufficient computer RAM.

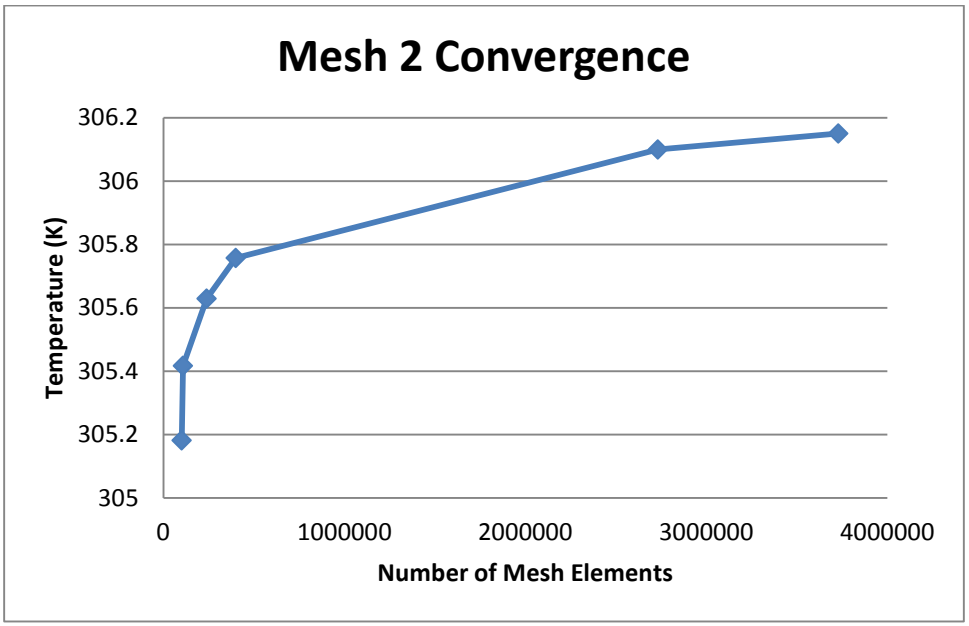

Fig. B2: Mesh convergence for Mesh 2. It appears that the solution is beginning to converge, but the converged solution requires too much time and memory to compute. The solution at the finest mesh shown took an excessive amount of time to calculate and will not be used for to calculate results for this report: instead, the third finest mesh on this graph was.

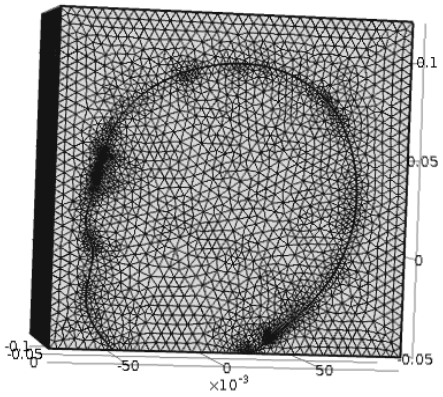

Fig. B1: Temperature mesh with maximum element size of 0.0054 m.

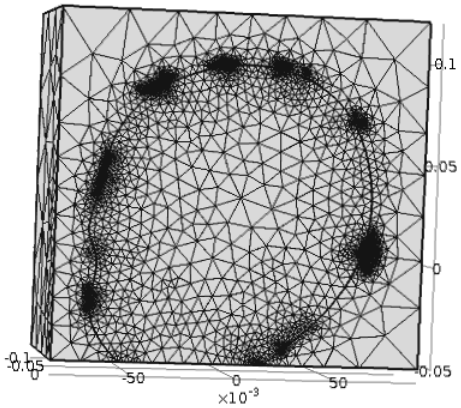

Fig. B2: Temperature mesh with maximum element size of 0.054 m. This is the coarsest mesh tested.

X. Appendix C: Implementation in COMSOL

Our model was run using two studies. One solved for the stationary mesh and solved for the steady state results for air flow and pressure using MUMPS. The second study solved for the temperature mesh and computer the transient heat transfer results using PARADISO. The solver parameters were kept at their default values.

XI. Appendix D: Results for Other Situations

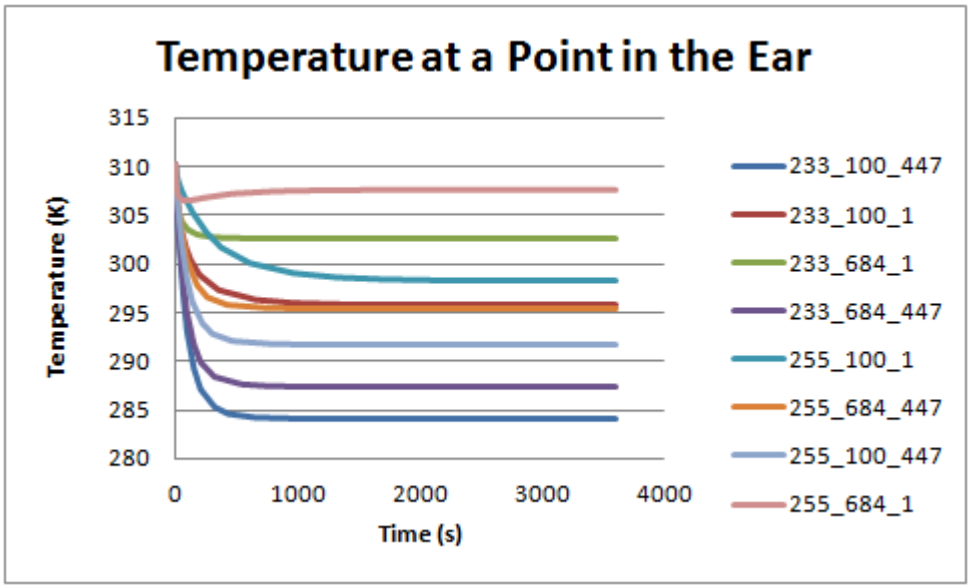

Fig. D1: Temperature profiles for all 8 situations. The properties are listed in the legend in the following order: Air temperature [K], radiative heat flux [W/m^2], wind speed [m/s]. Note that 447 corresponds to 4.47 m/s.

As one can see, lower air temperature is not necessarily predictive of lower ear temperatures under extreme conditions of Sun and wind (or lack thereof), since a higher radiative heat flux and lower wind speed both have a large effect on ear temperature and can still increase ear temperature appreciably.

References

1) Aguilar, G., Basu, R., Diaz, S. H., Laverniac, E. & Wong, B. J. F. (2002). Modeling the Thermal Response of Porcine Cartilage to Laser Irradiation. *Proc. SPIE, 4617,* 47-56. Retrieved from http://www.engr.ucr.edu/~gaguilar/PUBLICATIONS/P9.pdf

2) Average Wind Speeds. Retrieved from http://www.wrcc.dri.edu/htmlfiles/westwind.final.html

3) Bowman, H. F., Cravalho, E. G., & Woods, M. (1975). Theory, Measurement, and Application of Thermal Properties of Biomaterials. *Annual Review of Biophysics and Bioengineering, 4,* 43-80. DOI: 10.1146/annurev.bb.04.060175.000355

4) Crawford, C., Zafren, K. (2013). Frostbite. *UpToDate*. Retreived from http://www.uptodate.com/contents/frostbite

5) Datta, A., Rakesh, V. (2010). *An Introduction to Modeling of Transport Processes: Applications to Biomedical Systems.* Cambridge, NY: Cambridge University Press.

6) Elwassif, M. M., Kong, Q., Vazquez, M., Bikson, M. (2006). Bio-heat Transfer Model of Deep Brain Stimulation-induced Temperature Changes. *Journal of Neural Engineering, 3(4),* 306-315. DOI: 10.1088/1741-2560/3/4/008

7) Emanuel, D. C., Letowski, T. R. & Maroonroge, S. Basic Anatomy of the Hearing System. Retrieved from http://www.usaarl.army.mil/publications/HMD_Book09/files/Section%2015%20-%20Chapter%208%20Ear%20Anatomy.pdf

8) Mayo Clinic Staff (2014). Diseases and Conditions - Gangrene. *Mayo Clinic.* Retrieved from http://www.mayoclinic.org/diseases-conditions/gangrene/basics/definition/con-20031120

9) Miller, J. M., Ren, T. Y., Nuttall, A. L. (1995). Studies of Inner Ear Blood Flow in Animals and Human Beings. *Otolaryngol Head Neck Surgery, 112(1),* 101-113.

10) NOAA, National Weather Service Office of Climate, Water, and Weather Services (2013). NWS Winchill Chart. *National Weather Service.* Retrieved from http://www.nws.noaa.gov/os/windchill/index.shtml

11) Pediatric Orthopaedic Society of North America (2007). Frostbite. *American Academy of Orthopaedic Surgeons*. Retrieved from http://orthoinfo.aaos.org/topic.cfm?topic=a00193

12) Russell, R. (2010). Solar Radiation at Earth. *The National Earth Science Teachers Association.* Retrieved from http://www.windows2universe.org/earth/climate/sun_radiation_at_earth.html

13) Shelton, D. P. (2008). Air Properties: Temperature and Relative Humidity. *University of Nebraska-Lincoln Extension, Institute of Agriculture and Natural Resources.* Retrieved from http://www.ianrpubs.unl.edu/pages/publicationD.jsp?publicationId=1000

14) Shelquist, R. (1998). An Introduction to Air Density and Density Altitude Calculations. *Shelquist Engineering.* Retrieved from http://www.gribble.org/cycling/air_density.html

15) Shepherd, J. T., Rusch, N. J., Vanhoutte, P. M. (1983). Effect of Cold on the Blood Vessel Wall. *Gen Pharmacol, 14(1),* 61-64.

16) Urieli, I. (2014). Specific Heat Capacities of Air. *Ohio University.* Retrieved from http://www.ohio.edu/mechanical/thermo/property_tables/air/air_Cp_Cv.html

17) Vorvick, L. J. (2014). Body Temperature Normals. *U.S. National Library of Medicine.* Retrieved from http://www.nlm.nih.gov/medlineplus/ency/article/001982.htm

18) Yu, L. N., Liu, J. (2007). Entropy Generation Theory for Characterizing the Freezing and Thawing Injury of Biological Materials. *Forsch Ingenieurwes, 71,* 125-134. DOI: 10.1007/s10010-007-0051-y